

Development Of Analytical Model For Determination Of Degree Of Urbanisation Parameter Settings Of CCIR Model Based On Hata Model

Olutimo , Akinwale Lewis¹

Department of Mathematics, Lagos State University,
Lagos State , Nigeria
akinwale.olutimo@lasu.edu.ng

Enyenihi Henry Johnson²

Department of Electrical and Electronic Engineering,
Akwa Ibom State University Mkpatt Enin, Akwa
Ibom State
enyenihijohnson@aksu.edu.ng

Akpasam Joseph Ekanem³

Department of Electrical and Electronic Engineering,
Akwa Ibom State University Mkpatt Enin, Akwa Ibom State

Abstract—The Comité International des Radio-Communication (CCIR) path loss model and the Hata model pathloss estimations agree perfectly in the urban area for the frequency range of 150 MHz to 1500 MHz for which the models were originally designed. However, the two models' pathloss estimation differ significantly in other frequency range and for every other propagation environment. Accordingly, in this paper, development of an analytical model for determination of degree of urbanisation (DU) parameter settings of CCIR model based on Hata model is presented. The existing CCIR specification of DU for rural area is 3 % whereas the results in this paper show that for the rural area the degree of urbanization parameter (DU) decreases with frequency, from $DU = 1.783587\%$ at 150 MHz to $DU = 0.982767\%$ at 1500 MHz. Again, the results also show that for the suburban area the degree of urbanization parameter (DU) decreases with frequency in the frequency range of $150\text{ MHz} \leq f \leq 1500\text{ MHz}$ whereas the DU increases with frequency in the frequency range of $1500\text{ MHz} \leq f \leq 2000\text{ MHz}$. Furthermore, results show that for the urban area the degree of urbanization parameter (DU) decreases with frequency in all the frequency range of $150\text{ MHz} \leq f \leq 200\text{ MHz}$, $200\text{ MHz} \leq f \leq 1500\text{ MHz}$ and $1500\text{ MHz} \leq f \leq 2000\text{ MHz}$. In all, the results show that the degree of urbanization parameter (DU) varies with frequency and hence, the signal frequency must be considered in the estimation of the applicable value of degree of urbanization parameter value in the CCIR model.

Keywords: Pathloss, CCIR Model, Degree of Urbanisation, Attenuation, Hata Pathloss Model, Wireless Communication

1. Introduction

Generally, wireless communication path usually present some forms of signal degradation mechanisms such as obstructions in the signal path, adverse atmospheric conditions, interferences along with the inevitable free space propagation loss [1,2, 3,4, 5,6, 7,8, 9,10, 11,12, 13]. These degradations can result in diffraction loss, multipath loss, rain fading, and some other forms of losses [14,5,16,17,18,19,20,21,22,23,24,25,26,27,28,29,30].

Irrespective of whether the wireless link is for terrestrial or for satellite communication, appropriate estimation of the signal propagation losses is required [31,32,33,34,35, 36,37,38 ,39,40,41,42, 43, 44,45]. Accordingly, over the years, different pathloss models have been developed by experts in a bid to enable wireless communication system designers to account for the propagation losses that are prevalent in the propagation path of wireless communication links [46,7,48 49,50,51, 52, 53, 54,55,56,57,58,59,60].

Particularly, the Hata pathloss model was developed for urban environment and then modified to derive the versions for the rural and suburban area [61,62,63, 64, 65,66,67]. Originally, the Hata model was developed for the frequency range of 150 MHz to 1500 MHz [68,69,70,71]. However, it was later extended to the frequency range of 1500 MHz to 2000 MHz by some forms of modifications on the original Hata pathloss model [72,73,74, 75,76,77,78].

Furthermore, the Comité International des Radio-Communication (CCIR) developed a pathloss model that is similar to the Hata model for urban area but differs in the way it defines degree of urbanisation [79,80, 81,82,83,84]. While Hata model identifies and uses well defined analytical models to determine values applicable to urban area (large city), urban area (small city), suburban area and rural or open area, the CCIR model uses a parameter (DU) called degree of urbanization to differentiate the different areas. The degree of urbanization, DU parameter used in the CCIR pathloss model does not have any empirical guide for appropriate estimation of the value for different

categories of areas like the urban, suburban, and rural areas [85,86,87,88,89]. Fortunately, the similarity of CCIR model and Hata pathloss model can be used to provide a more accurate estimation of the urbanization, DU parameter value for each of the different terrains covered in the two pathloss models. Accordingly, in this paper, an approach for determination of the values of urbanization, DU parameter is presented. The study also considered the extended Hata model and the corresponding urbanization, DU parameter values for the extended Hata model was also derived.

2. Methodology

2.1. The Comité International des Radio-Communication (CCIR) Pathloss Model

The CCIR model is expressed as follows;

$$LP_{CCIR} = A + B * \log_{10}(d) - DU \quad (1)$$

where

$$A = 69.55 + 26.16 * \log_{10}(f) - 13.82 * \log_{10}(h_b) - a(h_m) \quad (2)$$

$$a(h_m) = [1.1 * \log_{10}(f) - 0.7] * h_m - [1.56 * \log_{10}(f) - 0.8] \quad (3)$$

$$B = 44.9 - 6.55 * \log_{10}(h_b) \quad (4)$$

$$E = 30 - 25(\log_{10}(DU)) \quad (5)$$

Where DU denotes the percentage of area that is covered by obstructions such as buildings. The frequency f is in MHz , the distance, d is in km while h_b and h_m are in meters. Also, the applicable frequency range is $150 \text{ MHz} \leq f \leq 1500 \text{ MHz}$. The applicable range of values for h_b , h_m and d are $30 \text{ m} \leq h_b \leq 200 \text{ m}$; $1 \text{ m} \leq h_m \leq 10 \text{ m}$ and $1 \text{ km} \leq d \leq 20 \text{ km}$.

Available literatures state that for urban area, $DU \geq 16\%$, for suburban area, $DU \approx 8\%$ and for rural area, $DU \approx 3\%$. The frequency f is in MHz , the distance, d is in km while h_b and h_m are in meters. Also, the applicable frequency range is $150 \text{ MHz} \leq f \leq 1000 \text{ MHz}$. The applicable range of values for h_b , h_m and d are $30 \text{ m} \leq h_b \leq 200 \text{ m}$; $1 \text{ m} \leq h_m \leq 10 \text{ m}$ and $1 \text{ km} \leq d \leq 20 \text{ km}$.

2.2 The Hata Pathloss Model

Similar to the CCIR model, the Hata pathloss models for the different categories of areas based on the degree of urbanisation are expressed as follows:

$$LP_{HATA(urban)} = A + B * \log_{10}(d) \quad \text{for Urban Area (small city or large city)} \quad (6)$$

$$LP_{HATA(suburban)} = A + B * \log_{10}(d) - C \quad \text{for Suburban Area} \quad (7)$$

$$LP_{HATA(open/rural)} = A + B * \log_{10}(d) - D \quad \text{for Open Area/Rural} \quad (8)$$

$$A = 69.55 + 26.16 * \log_{10}(f) - 13.82 * \log_{10}(h_b) - a(h_m) \quad (9)$$

$$B = 44.9 - 6.55 * \log_{10}(h_b) \quad (10)$$

$$C = 5.4 + 2 * \left[\log_{10} \left(\frac{f}{28} \right) \right]^2 \quad (11)$$

$$D = 40.94 + 4.78 * [\log_{10}(f)]^2 - 18.33 * \log_{10}(f) \quad (12)$$

$$a(h_m) = [1.1 * \log_{10}(f) - 0.7] * h_m - [1.56 * \log_{10}(f) - 0.8] \quad (14)$$

$$a(h_m) = 8.28 * [\log_{10}(1.54 * h_m)]^2 - 1.1 \quad \text{for large city } 150 \text{ MHz} \leq f \leq 200 \text{ MHz} \quad (15)$$

$$a(h_m) = 3.2 * [\log_{10}(11.75 * h_m)]^2 - 4.97 \quad \text{for large city } 200 \text{ MHz} \leq f \leq 1500 \text{ MHz} \quad (16)$$

Where the frequency f is in MHz, the distance, d is in km while h_b and h_m are in meters. Also, the applicable frequency range is $150 \text{ MHz} \leq f \leq 1500 \text{ MHz}$. The applicable range of values for h_b , h_m and d are $30 \text{ m} \leq h_b \leq 200 \text{ m}$; $1 \text{ m} \leq h_m \leq 10 \text{ m}$ and $1 \text{ km} \leq d \leq 20 \text{ km}$.

2.3 Extended Hata Model

The Hata pathloss model was designed for frequency range of $150 \text{ MHz} \leq f \leq 1500 \text{ MHz}$. In order to use the Hata model in the frequency range of $1500 \text{ MHz} \leq f \leq 2000 \text{ MHz}$ some modifications were made on the classical Hata model. The modified Hata model for the extended frequency range of $1500 \text{ MHz} \leq f \leq 2000 \text{ MHz}$ is called the extended Hata model and it is expressed as follows;

$$LP_{EX_HATA(urban)} = A_{EX} + B * \log_{10}(d) + 3 \quad \text{for } 1500 \text{ MHz} \leq f \leq 2000 \text{ MHz} \quad (17)$$

$$LP_{EX_HATA(suburban)} = A_{EX} + B * \log_{10}(d) \quad \text{for } 1500 \text{ MHz} \leq f \leq 2000 \text{ MHz} \quad (18)$$

where

$$A_{EX} = 46.33 + 33.9 * \log_{10}(f) - 13.82 * \log_{10}(h_b) - a(h_m) \quad (19)$$

$$B_{EX} = B = 44.9 - 6.55 * \log_{10}(h_b) \quad (20)$$

The expressions for $a(h_m)$ and B still applies to the extended Hata model.

2.4 Development of the model for computing the degree of urbanisation (DU) parameter

In order to determine the optimal value of the degree of urbanisation (DU) parameter, the pathloss estimated using the CCIR model for urban area is compared with the pathloss estimated using the Hata model for urban area. The initial value of 16 % was selected for DU and then, Microsoft Excel Solver add-in tool is used to determine the optimal value of the degree of urbanisation (DU) parameter for the urban area at the selected frequency. The procedure is repeated for different signal frequencies and communication ranges, and also for different transmitter-receiver antenna height differentials. Afterwards, an analytical model is fitted on the generated values of DU versus frequency for the urban area. The entire procedure is repeated for the suburban area and also for the rural area.

In order to understand the relationship between the degree of urbanisation and the resultant pathloss in the various categories of areas they apply, the plot of pathloss at selected frequencies in each of the applicable frequency ranges for the different areas are presented from Figure 1 to Figure 9. The pathloss for the rural area are presented in Figure 1 and Figure 2 and the two graphs show that the

CCIR model prediction of pathloss for the rural area is above that of the Hata model when the 3 % is used to compute the degree of urbanisation for rural area.

The pathloss for the suburban area are presented in Figure 3, Figure 4 and Figure 5 and the three graphs show that the CCIR model prediction of pathloss for the suburban area is approximately the same as that of Hata model at the lower frequency of 150 MHz. However, at higher frequencies, the CCIR model predictions differ from that of the Hata model. Essentially, there is frequency dependence of the degree of urbanisation which is not captured in the existing specification for the CCIR model.

Again, the pathloss for the urban area are presented in Figure 6, Figure 7, Figure 8 and Figure 9 and the four graphs show that the CCIR model prediction of pathloss for the urban area is approximately the same as that of Hata model at the frequency range from 150 MHz to 1500 MHz. However, at higher frequencies above 1500 MHz (which is the region for the extended Hata model), the CCIR model predictions differ from that of the extended Hata model. Essentially, the existing degree of urbanisation for CCIR model was determined based on the Hata pathloss model for the urban area. However, degree of urbanisation for the the extended Hata model is not yet established.

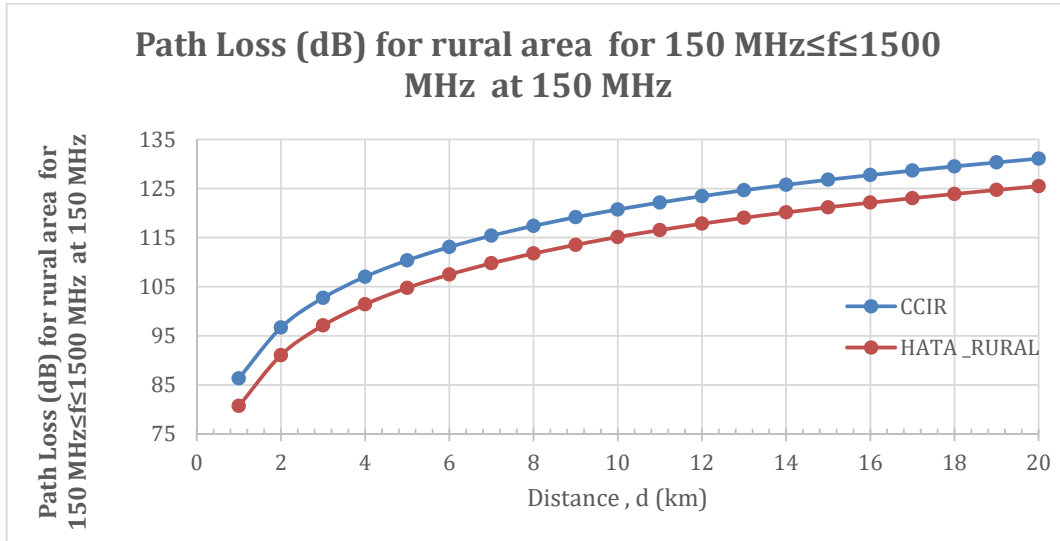


Figure 1 Pathloss (dB) for rural area at frequency of 150 MHz for the range 150 MHz ≤ f ≤ 1500 MHz

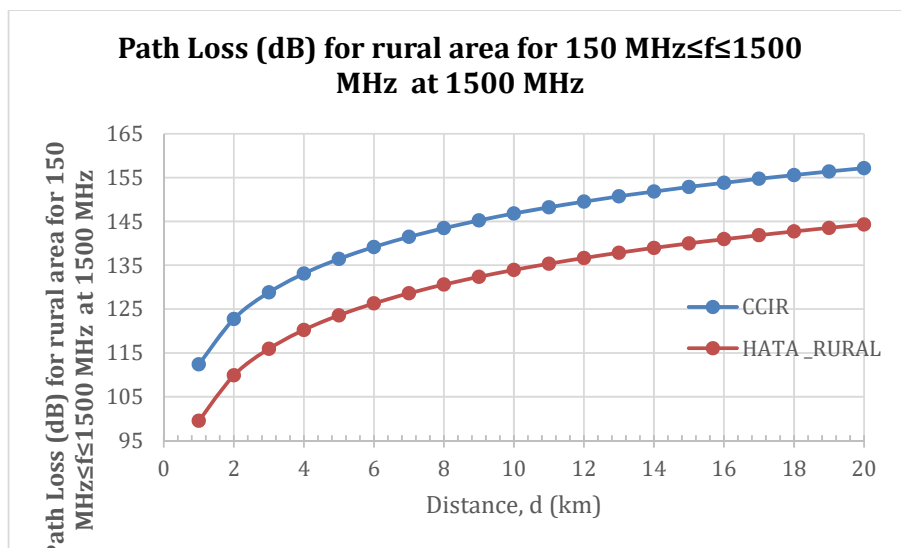


Figure 2 Pathloss (dB) for rural area at 1500 MHz for the range 150 MHz ≤ f ≤ 1500 MHz

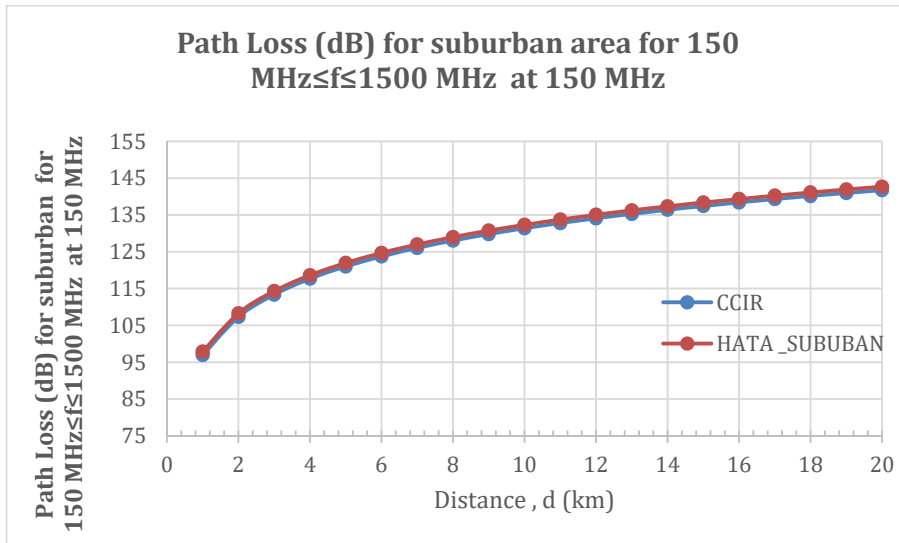


Figure 3 Pathloss (dB) for suburban area at 150 MHz for the range 150 MHz ≤ f ≤ 1500 MHz

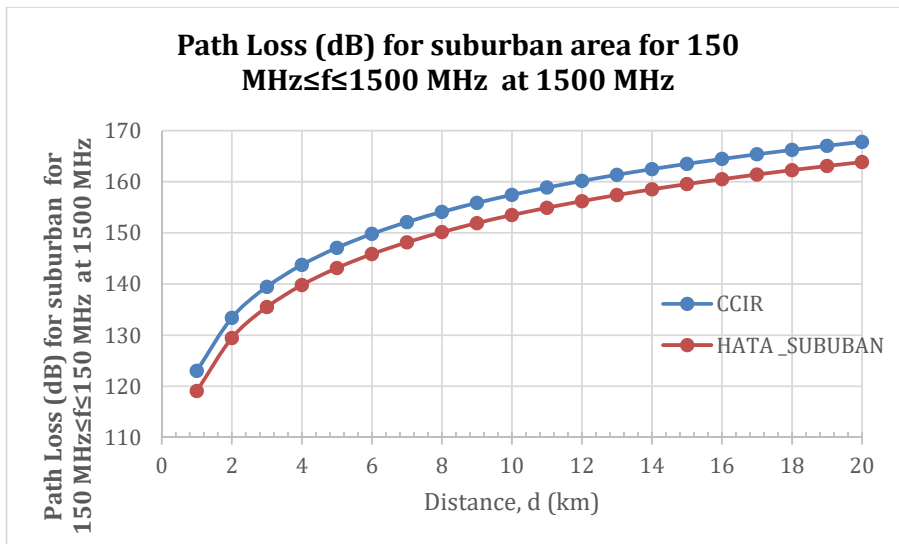


Figure 4 Pathloss (dB) for suburban area at 1500 MHz for the range 1500 MHz ≤ f ≤ 1500 MHz

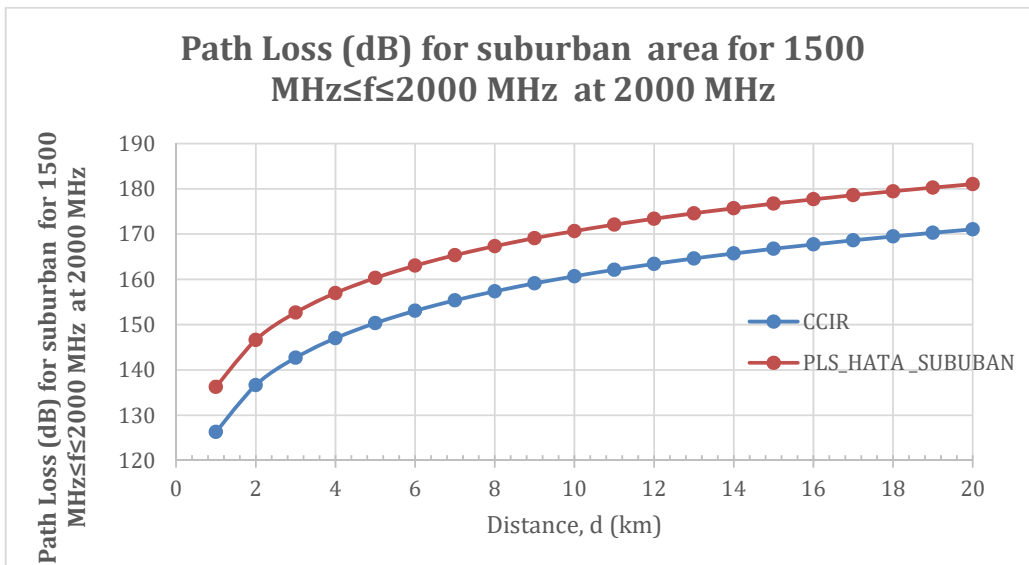


Figure 5 Pathloss (dB) for suburban area at 2000 MHz for the range 1500 MHz ≤ f ≤ 2000 MHz

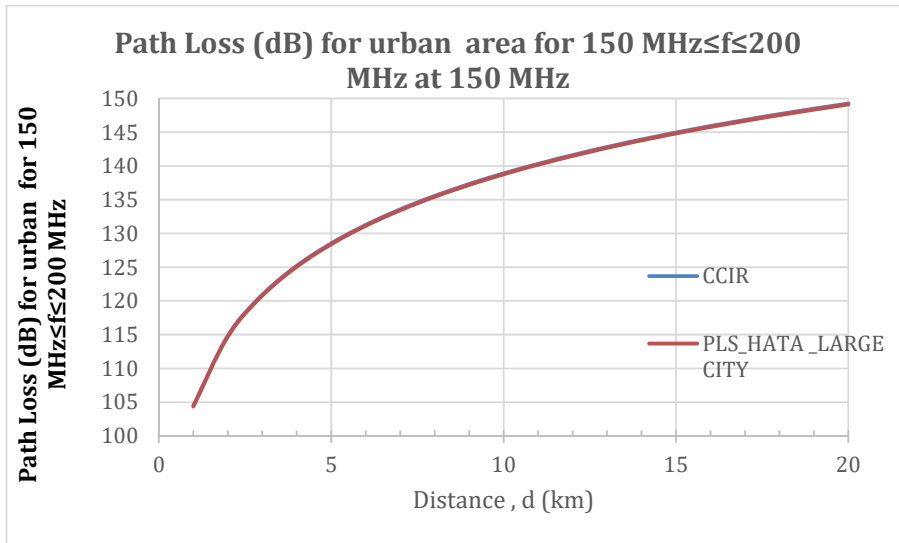


Figure 6 Pathloss (dB) for urban area at 150 MHz for the range 150 MHz ≤ f ≤ 200 MHz

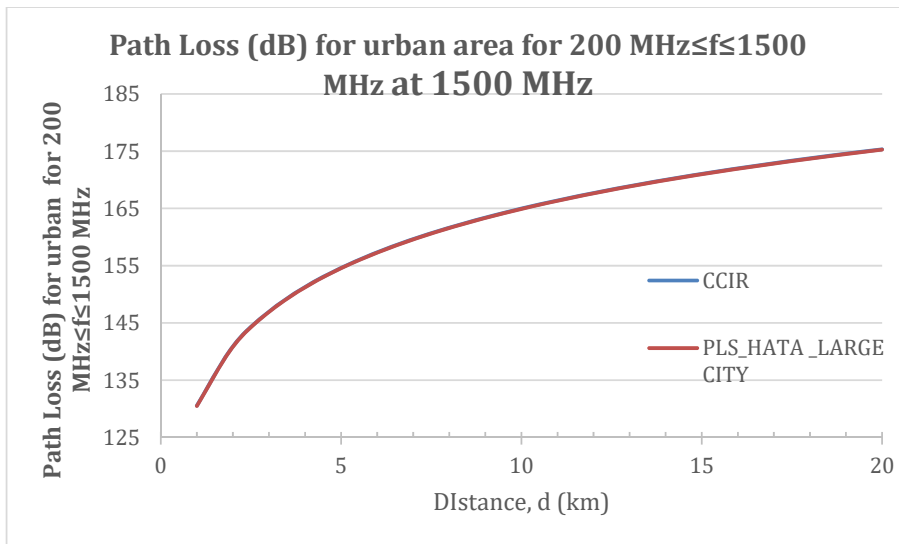


Figure 7 Pathloss (dB) for urban area at 1500 MHz for the range 200 MHz ≤ f ≤ 1500 MHz

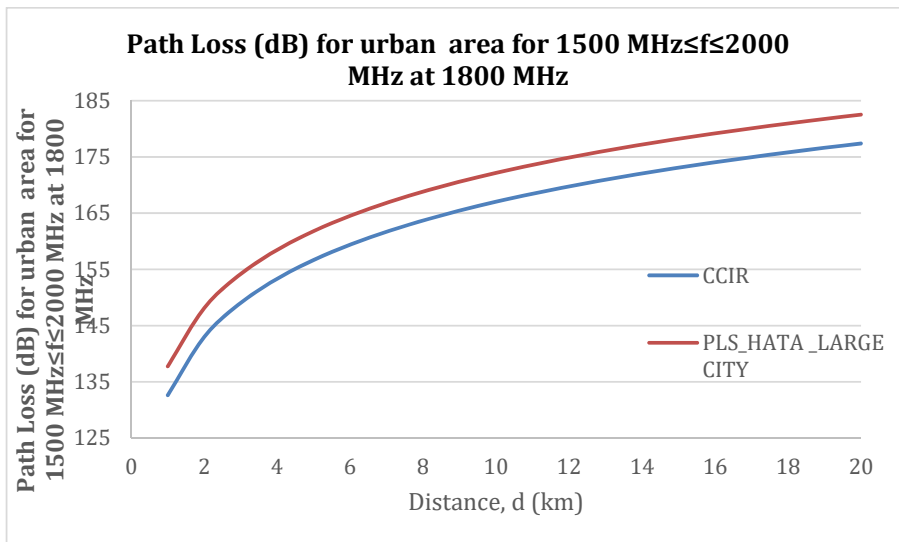


Figure 8 Pathloss (dB) for urban area at 1800 MHz for the range 1500 MHz ≤ f ≤ 2000 MHz

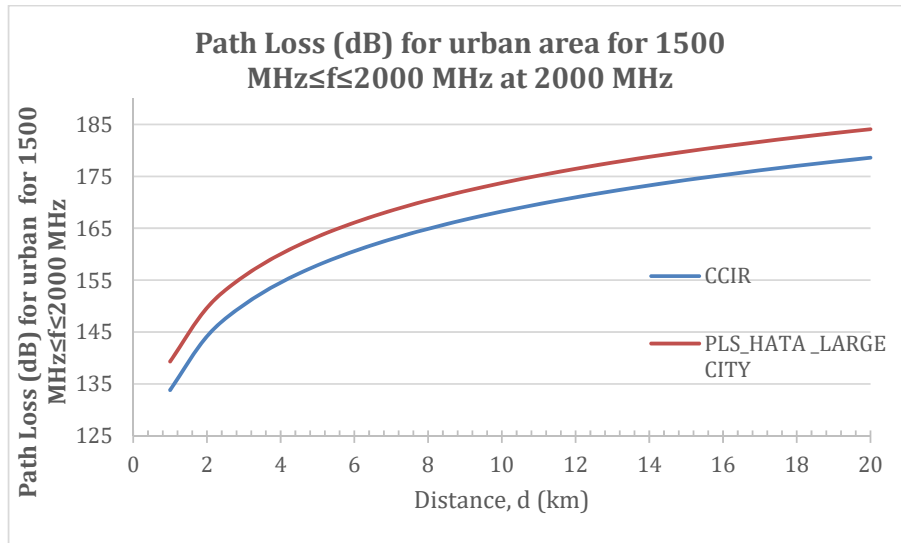


Figure 9 Pathloss (dB) for urban area at 2000 MHz for the range 1500 MHz ≤ f ≤ 2000 MHz

3. Results and Conclusion

The degree of urbanisation parameter (DU) was determined for the three categories of areas, the rural, the suburban and the urban area. The Microsoft Excel add-in Solver tool was used to determine the optimal value of DU that will minimize the error between the Hata model predicted pathloss and the CCIR predicted pathloss for each of the area and frequency range.

The results for the degree of urbanization, DU (%) for rural area for the frequency range of 150 MHz ≤ f ≤ 1500 MHz are shown in Table 1 and Figure 10. Based on the results in Table 1, a quadratic analytical model that can be used to select appropriate DU value for CCIR model in the rural area is given in terms of the signal frequency, f as;

$$DU = 0.0000004f^2 - 0.0012532f + 1.9625673 \quad (21)$$

Where f is in MHz.

Table 1 The results for the degree of urbanization, DU (%) for rural area for the frequency range of 150 MHz ≤ f ≤ 1500 MHz

Frequency, f (MHz)	Degree of urbanisation (DU) (%) for Rural area for 150 MHz ≤ f ≤ 1500 MHz	RMSE (dB)
150	1.789	4.76E-07
160	1.777	8.17E-07
170	1.764	7.03E-07
180	1.752	1.34E-06
190	1.739	1.35E-06
200	1.726	1.62E-07
300	1.605	4.39E-06
600	1.329	9.91E-07
900	1.147	1.05E-07
1200	1.017	2.76E-07
1500	0.917	8.19E-06
Mean	1.506	1.71E-06

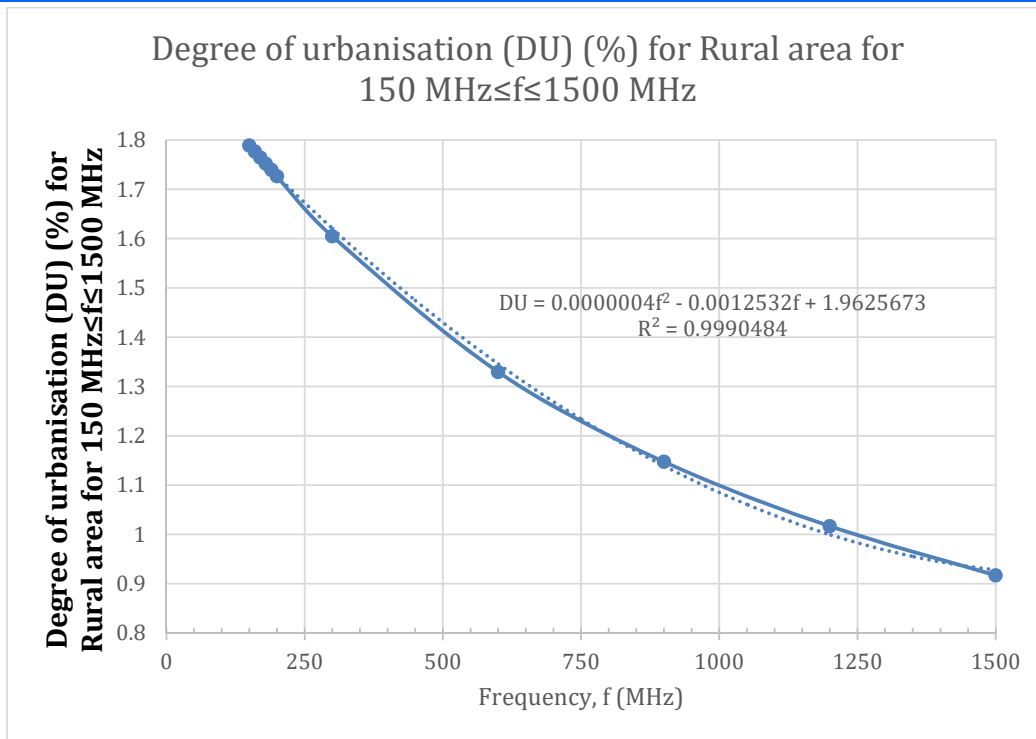


Figure 10 The degree of urbanization , DU (%) for rural area for the frequency range of 150 MHz ≤ f ≤ 1500 MHz

The results for the degree of urbanization, DU (%) for suburban area for the frequency range of 150 MHz ≤ f ≤ 1500 MHz are shown in Table 2 and Figure 11. Based on the results in Table 2, a quadratic analytical model that can be used to select appropriate DU value for CCIR model in the suburban area in the frequency range of 150 MHz ≤ f ≤ 1500 MHz is given in terms of the signal frequency, f as;

$$DU = 0.0000015f^2 - 0.0047182f + 9.3120221 \quad (22)$$

Where f is in MHz. Again, the results for the degree of urbanization, DU (%) for suburban area for the frequency range of 1500 MHz ≤ f ≤ 2000 MHz are shown in Table 3 and Figure 12. Based on the results in Table 3, a quadratic analytical model that can be used to select appropriate DU value for CCIR model in the suburban area in the frequency range of 1500 MHz ≤ f ≤ 2000 MHz is given in terms of the signal frequency, f as;

$$DU = -0.00000068f^2 + 0.00578263f + 11.18623102 \quad (23)$$

Table 2 The results for the degree of urbanization, DU (%) for suburban area for the frequency range of 150 MHz ≤ f ≤ 1500 MHz

Frequency, f (MHz)	Degree of urbanisation (DU) (%) for suburban area for 150 MHz ≤ f ≤ 1500 MHz	RMSE (dB)
150	8.7396	3.31E-07
170	8.6083	8.77E-07
190	8.4855	2.84E-08
210	8.3703	1.17E-07
250	8.1598	4.01E-07
300	7.9275	1.41E-06
600	6.9547	1.05E-06
900	6.3430	1.40E-09
1200	5.9009	1.04E-05
1500	5.5573	5.57E-07
Mean	7.5047	1.52E-06

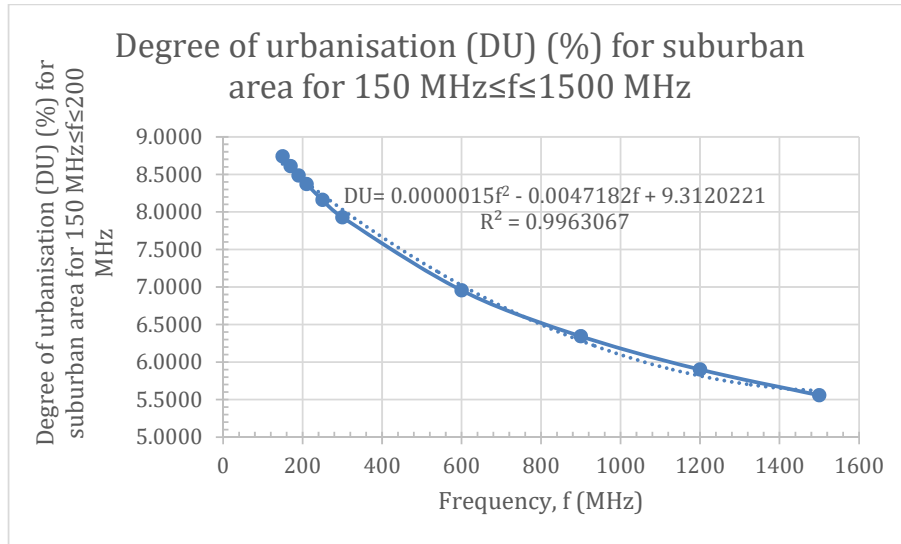


Figure 11 The degree of urbanization , DU (%) for suburban area for the frequency range of 150 MHz ≤ f ≤ 1500 MHz

Table 3 The degree of urbanization , DU (%) for suburban area for the frequency range of 1500 MHz ≤ f ≤ 2000 MHz

Frequency, f (MHz)	Degree of urbanisation (DU) (%) for suburban area for 1500 MHz ≤ f ≤ 2000 MHz	RMSE (dB)
1500	18.3366	3.68E-08
1600	18.7066	8.76E-06
1700	19.0611	5.02E-07
1800	19.4014	4.54E-06
1900	19.7289	3.83E-08
2000	20.0447	5.29E-06
Mean	19.2132	3.19E-06

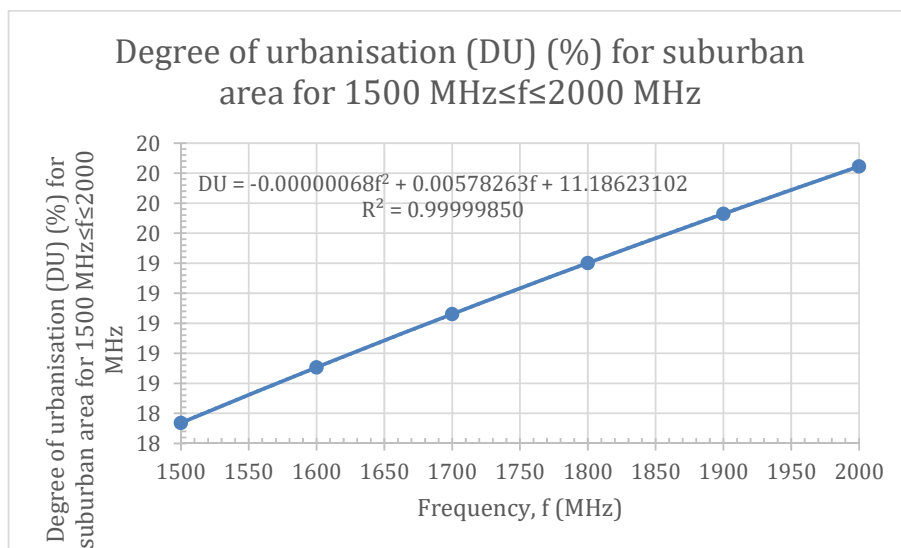


Table 12 The degree of urbanization , DU (%) for suburban area for the frequency range of 1500 MHz ≤ f ≤ 2000 MHz

The results for degree of urbanization , DU (%) for urban area for the frequency range of 150 MHz ≤ f ≤ 200 MHz are shown in Table 4 and Figure 13. Based on the results in Table 4, a quadratic analytical model that can be used to select appropriate DU value for CCIR model in the urban area in the frequency range of 150 MHz ≤ f ≤ 200 MHz is given in terms of the signal frequency, f as;

$$DU = -0.000001f^2 + 0.000654f + 15.700734 \quad (24)$$

Where f is in MHz. Again, the results for degree of urbanization , DU (%) for urban area for the frequency range of 200 MHz ≤ f ≤ 1500 MHz are shown in Table 5 and Figure 14. Based on the results in Table 5, a quadratic analytical model that can be used to select appropriate DU

value for CCIR model in the suburban area in the frequency range of 200 MHz ≤ f ≤ 1500 MHz is given in terms of the signal frequency, f as;

$$DU = -0.00000006f^2 + 0.00018774f + 15.75585658 \quad (25)$$

Furthermore, the results for degree of urbanization , DU (%) for urban area for the frequency range of 1500 MHz ≤ f ≤ 2000 MHz are shown in Table 6 and Figure 15. Based on the results in Table 6, a quadratic analytical model that can be used to select appropriate DU value for CCIR model in the suburban area in the frequency range of 1500 MHz ≤ f ≤ 2000 MHz is given in terms of the signal frequency, f as;

$$DU = -0.0000009f^2 + 0.0077249f + 14.6958400 \quad (26)$$

Table 4 The degree of urbanization , DU (%) for urban area for the frequency range of 150 MHz ≤ f ≤ 200 MHz

Frequency, f (MHz)	Degree of urbanisation (DU) (%) for urban area for 150 MHz ≤ f ≤ 200 MHz	RMSE (dB)
150	15.77774	1.04E-07
160	15.7814	7.75E-08
170	15.78485	1.39E-07
180	15.78809	2.12E-06
190	15.79117	2.57E-08
200	15.79409	1.54E-06
Mean	15.78622	6.68E-07

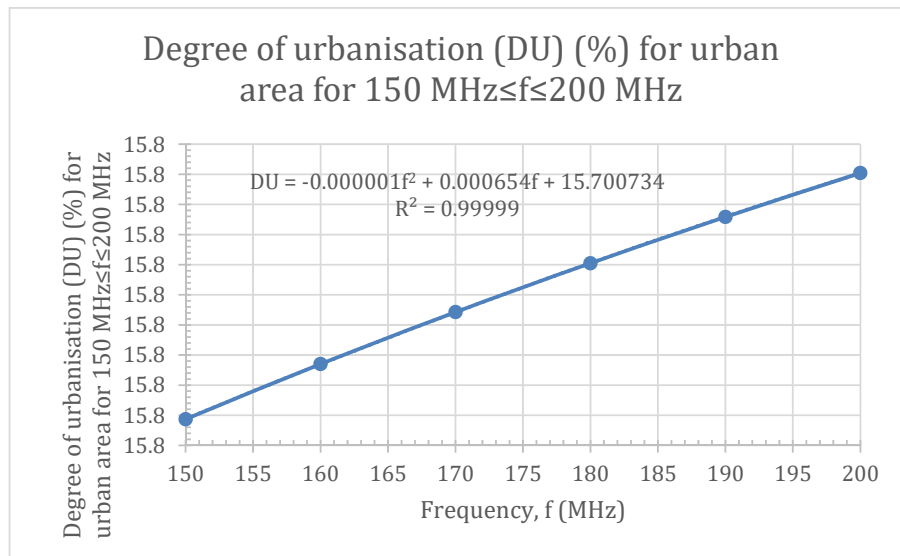


Figure 13 The degree of urbanization , DU (%) for urban area for the frequency range of 150 MHz ≤ f ≤ 200 MHz

Table 5 The degree of urbanization , DU (%) for urban area for the frequency range of 200 MHz≤f≤1500 MHz

Frequency, f (MHz)	Degree of urbanisation (DU) (%) for urban area for 200 MHz≤f≤1500 MHz	RMSE (dB)
200	15.78775	5.43E-06
500	15.83991	7.07E-06
700	15.85912	1.85E-06
900	15.87347	2.60E-06
1100	15.88493	9.66E-06
1300	15.8945	9.78E-07
1500	15.90269	2.33E-07
Mean	15.8632	3.97E-06

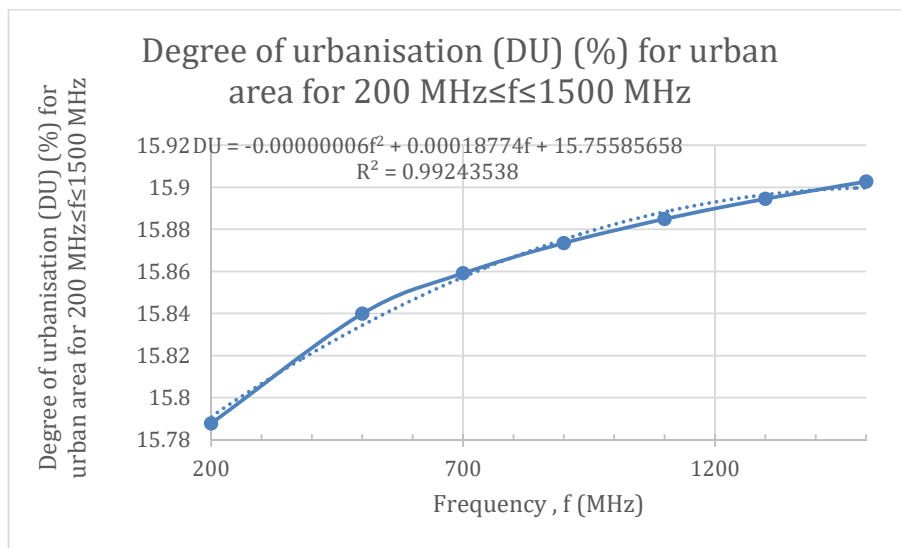


Figure 14 The degree of urbanization , DU (%) for urban area for the frequency range of 200 MHz≤f≤1500 MHz

Table 6 The degree of urbanization , DU (%) for urban area for the frequency range of 1500 MHz≤f≤2000 MHz

Frequency, f (MHz)	Degree of urbanisation (DU) (%) for urban area for 1500 MHz≤f≤2000 MHz	RMSE (dB)
1500	24.254	1.17E-06
1600	24.750	5.91E-06
1700	25.224	3.81E-06
1800	25.680	3.49E-08
1900	26.118	6.09E-06
2000	26.541	1.12E-07
Mean	25.428	2.85E-06

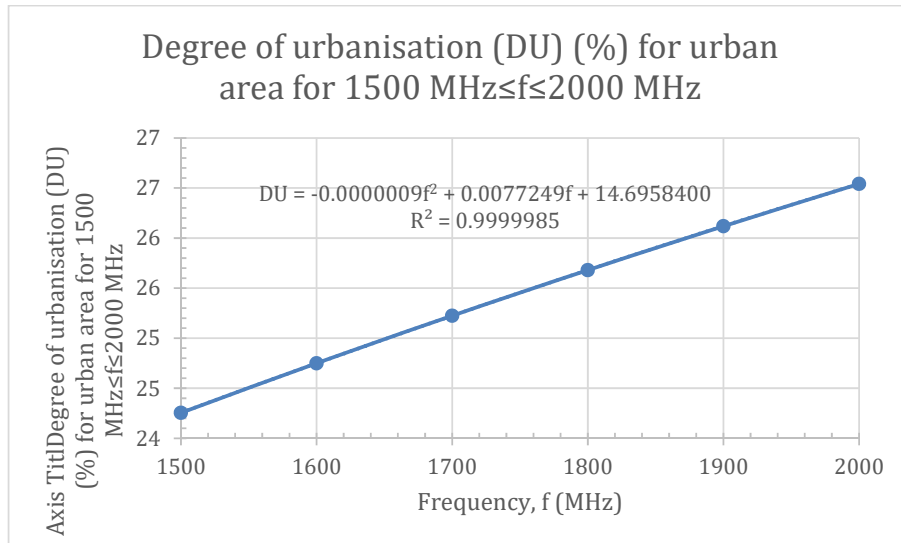


Figure 15 The degree of urbanization, DU (%) for urban area for the frequency range of 1500 MHz ≤ f ≤ 2000 MHz

The analytical models for the degree of urbanization parameter (DU) were used to determine the DU values for rural area, suburban area and urban area and for frequencies. The existing degree of urbanization and the model estimated degree of urbanization and the corresponding RMSE value of pathloss estimation for rural area at 1500 MHz for the frequency range 150 MHz ≤ f ≤ 1500 MHz are shown in Table 7 and Figure 16. The results show that for the rural area the degree of urbanization parameter (DU) decreases with frequency. The existing degree of urbanization and the model estimated degree of urbanization and the corresponding RMSE value of pathloss estimation for suburban area for the frequency range of 150 MHz ≤ f ≤ 1500 MHz and 1500 MHz ≤ f ≤ 2000 MHz are shown in Table 8 and Figure 17. The results show that for the suburban area the degree of

urbanization parameter (DU) decreases with frequency in the frequency range of 150 MHz ≤ f ≤ 1500 MHz whereas the DU increases with frequency in the frequency range of 1500 MHz ≤ f ≤ 2000 MHz. The existing degree of urbanization and the model estimated degree of urbanization and the corresponding RMSE value of pathloss estimation for urban area for the frequency range of 150 MHz ≤ f ≤ 200 MHz, 200 MHz ≤ f ≤ 1500 MHz and 1500 MHz ≤ f ≤ 2000 MHz are shown in Table 9 and Figure 18. The results show that for the urban area the degree of urbanization parameter (DU) decreases with frequency in all the frequency range of 150 MHz ≤ f ≤ 200 MHz, 200 MHz ≤ f ≤ 1500 MHz and 1500 MHz ≤ f ≤ 2000 MHz.

Table 7 The existing degree of urbanization and the model estimated degree of urbanization and the corresponding RMSE value of pathloss estimation for rural area at 1500 MHz for the frequency range 150 MHz ≤ f ≤ 1500 MHz

Frequency range in MHz	Selected frequency in MHz for the test	Existing urbanization parameter (DU) value in %	The pathloss RMSE in dB based on the existing DU value	Improved urbanization parameter (DU) value in %	The pathloss RMSE in dB based on the improved DU value
150 MHz ≤ f ≤ 1500 MHz	150	3	5.615362	1.783587	0.03031
150 MHz ≤ f ≤ 1500 MHz	500	3	8.21553	1.435967	0.216112
150 MHz ≤ f ≤ 1500 MHz	1000	3	10.89803	1.109367	0.096884
150 MHz ≤ f ≤ 1500 MHz	1500	3	12.86879	0.982767	0.752031

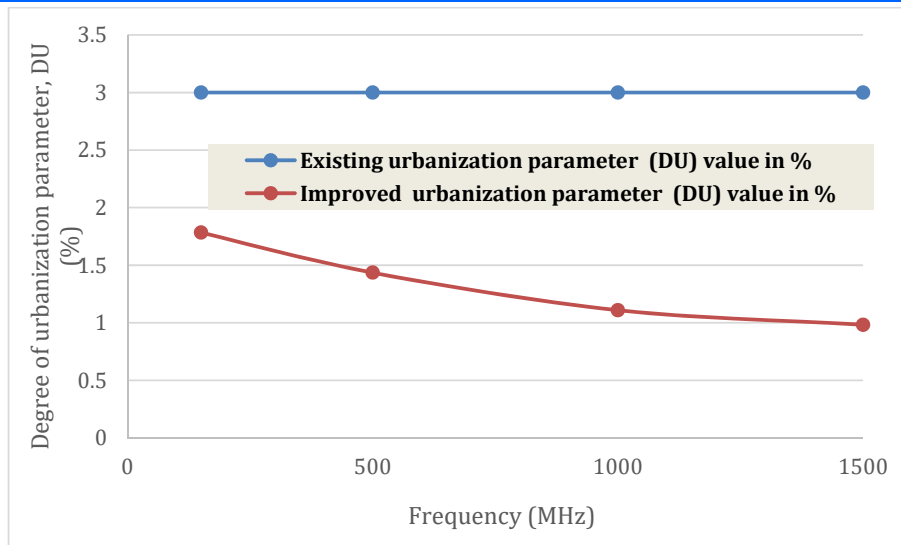


Figure 16 The existing degree of urbanization and the model estimated degree of urbanization for rural area at 1500 MHz for the frequency range $150 \text{ MHz} \leq f \leq 1500 \text{ MHz}$

Table 8 The existing degree of urbanization and the model estimated degree of urbanization and the corresponding RMSE value of pathloss estimation for suburban area for the frequency range of $150 \text{ MHz} \leq f \leq 1500 \text{ MHz}$ and $1500 \text{ MHz} \leq f \leq 2000 \text{ MHz}$

Frequency range in MHz	Selected frequency in MHz for the test	Existing urbanization parameter (DU) value in %	The pathloss RMSE in dB based on the existing DU value	Improved urbanization parameter (DU) value in %	The pathloss RMSE in dB based on the improved DU value
$150 \text{ MHz} \leq f \leq 1500 \text{ MHz}$	150	8	0.960063024	8.638042	0.12693
$150 \text{ MHz} \leq f \leq 1500 \text{ MHz}$	1500	8	3.955669887	5.609722	0.101954
$1500 \text{ MHz} \leq f \leq 2000 \text{ MHz}$	1700	8	9.426424977	19.0515	0.005444
$1500 \text{ MHz} \leq f \leq 2000 \text{ MHz}$	2000	8	9.972722492	20.03149	0.00714

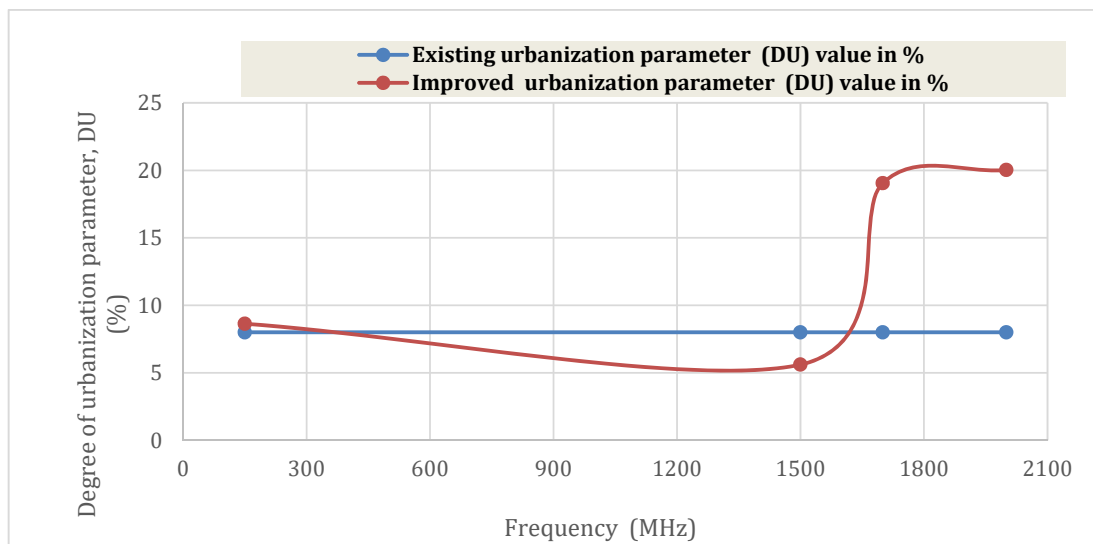


Figure 17 The existing degree of urbanization and the model estimated degree of urbanization for suburban area for the frequency range of $150 \text{ MHz} \leq f \leq 1500 \text{ MHz}$ and $1500 \text{ MHz} \leq f \leq 2000 \text{ MHz}$

Table 9 The existing degree of urbanization and the model estimated degree of urbanization and the corresponding RMSE value of pathloss estimation for urban area for the frequency range of $150 \text{ MHz} \leq f \leq 200 \text{ MHz}$, $200 \text{ MHz} \leq f \leq 1500 \text{ MHz}$ and $1500 \text{ MHz} \leq f \leq 2000 \text{ MHz}$

Frequency range in MHz	Selected frequency in MHz for the test	Existing urbanization parameter (DU) value in %	The pathloss RMSE in dB based on the existing DU value	Improved urbanization parameter (DU) value in %	The pathloss RMSE in dB based on the improved DU value
$150 \text{ MHz} \leq f \leq 200 \text{ MHz}$	150	16	0.151881	15.77633	0.000967
$150 \text{ MHz} \leq f \leq 200 \text{ MHz}$	200	16	0.140636	15.79153	0.001756
$200 \text{ MHz} \leq f \leq 1500 \text{ MHz}$	300	16	0.12914	15.80678	0.002776
$200 \text{ MHz} \leq f \leq 1500 \text{ MHz}$	1500	16	0.066232	15.90247	0.000155
$1500 \text{ MHz} \leq f \leq 2000 \text{ MHz}$	1800	16	5.136703	25.68466	0.002143
$1500 \text{ MHz} \leq f \leq 2000 \text{ MHz}$	2000	16	5.494984	26.54564	0.001846

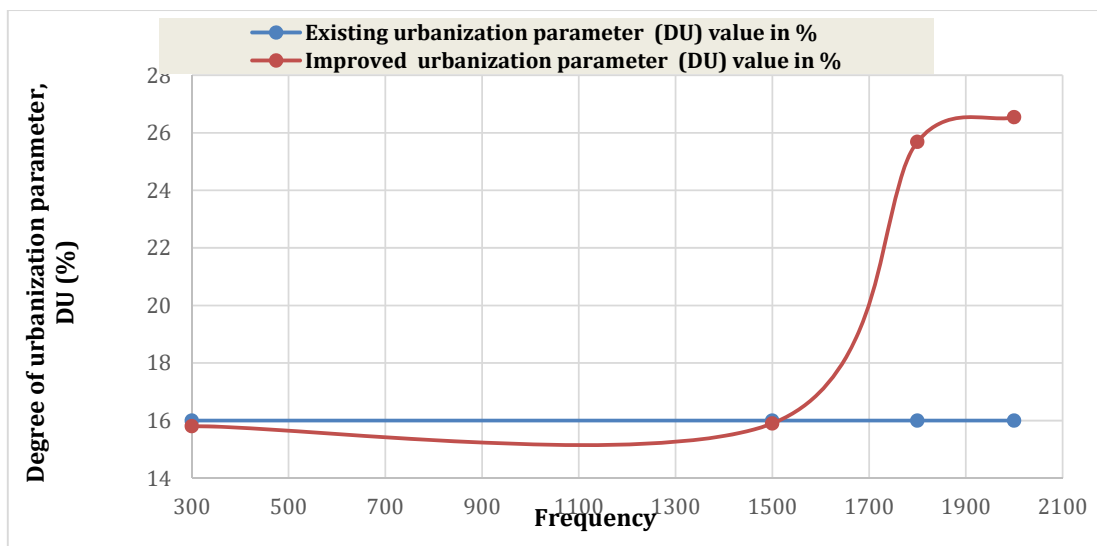


Figure 18 The existing degree of urbanization and the model estimated degree of urbanization for urban area for the frequency range of $150 \text{ MHz} \leq f \leq 200 \text{ MHz}$, $200 \text{ MHz} \leq f \leq 1500 \text{ MHz}$ and $1500 \text{ MHz} \leq f \leq 2000 \text{ MHz}$

4. Conclusion

An approach for selection of appropriate value of degree of urbanization parameter (DU) for the CCIR pathloss model is presented. The procedure adopted involve comparison of the pathloss estimation based on the existing values of CCIR model degrees of urbanisation specification for different signal propagation environments with the pathloss estimated by Hata model for the corresponding propagation environments. The results show that the Hata model and CCIR model specifications agreed perfectly in their pathloss estimation for the urban region for frequency range of 150 MH to 1500 MHz. However, the two models' pathloss estimation differ significantly in other frequency range and for every other propagation environment. Accordingly, analytical models were developed to estimate appropriate degree of urbanization parameter (DU) value that aligns the pathloss estimation of the two models in all the frequency range and propagation environments they are

designed to operate. The overall results show that the degree of urbanization parameter (DU) varies with frequency.

References

1. Kedar, D., & Arnon, S. (2004). Urban optical wireless communication networks: the main challenges and possible solutions. *IEEE Communications Magazine*, 42(5), S2-S7.
2. Akaninyene B. Obot , **Ozuomba Simeon** and Afolanya J. Jimoh (2011); "Comparative Analysis Of Pathloss Prediction Models For Urban Macrocellular" *Nigerian Journal of Technology (NIJOTECH)* Vol. 30, No. 3 , October 2011 , PP 50 – 59
3. Sklar, B. (1997). Rayleigh fading channels in mobile digital communication systems. I. Characterization. *IEEE Communications magazine*, 35(7), 90-100.

4. Akaninyene B. Obot , Ozuomba Simeon and Kingsley M. Udofia (2011); "Determination Of Mobile Radio Link Parameters Using The Path Loss Models" *NSE Technical Transactions , A Technical Journal of The Nigerian Society Of Engineers*, Vol. 46, No. 2 , April - June 2011 , PP 56 – 66.
5. Tian, Y., Xu, K., & Ansari, N. (2005). TCP in wireless environments: problems and solutions. *IEEE Communications Magazine*, 43(3), S27-S32.
6. Njoku Chukwudi Aloziem, **Ozuomba Simeon**, Afolayan J. Jimoh (2017) Tuning and Cross Validation of Blomquist-Ladell Model for Pathloss Prediction in the GSM 900 Mhz Frequency Band , *International Journal of Theoretical and Applied Mathematics*
7. Kalu, C., Ozuomba, Simeon. & Udofia, K. (2015). Web-based map mashup application for participatory wireless network signal strength mapping and customer support services. *European Journal of Engineering and Technology*, 3 (8), 30-43.
8. Tse, D., & Viswanath, P. (2005). *Fundamentals of wireless communication*. Cambridge university press.
9. **Ozuomba, Simeon**, Johnson, E. H., & Udoiwod, E. N. (2018). Application of Weissberger Model for Characterizing the Propagation Loss in a Gliricidia sepium Arboretum. *Universal Journal of Communications and Network*, 6(2), 18-23.
10. Ricklin, J. C., Hammel, S. M., Eaton, F. D., & Lachinova, S. L. (2006). Atmospheric channel effects on free-space laser communication. *Journal of Optical and Fiber Communications Reports*, 3(2), 111-158.
11. Constance, Kalu, **Ozuomba Simeon**, and Ezuruike Okafor SF. (2018). Evaluation of the Effect of Atmospheric Parameters on Radio Pathloss in Cellular Mobile Communication System. Evaluation, 5(11). *Journal of Multidisciplinary Engineering Science and Technology (JMEST) Vol. 5 Issue 11, November - 2018*
12. Uwaechia, A. N., & Mahyuddin, N. M. (2020). A comprehensive survey on millimeter wave communications for fifth-generation wireless networks: Feasibility and challenges. *IEEE Access*, 8, 62367-62414.
13. Kalu Constance, **Ozuomba Simeon**, Umana, Sylvester Isreal (2018). Evaluation of Walficsh-Bertoni Path Loss Model Tuning Methods for a Cellular Network in a Timber Market in Uyo. *Journal of Multidisciplinary Engineering Science Studies (JMESS) Vol. 4 Issue 12, December – 2018*
14. Adeogun, C. (2022). LOS Signal Path Loss at a Frequency of 10.6 GHz During Rain & Harmattan in Lagos, Nigeria.
15. Imoh-Etefia, Ubon Etefia, **Ozuomba Simeon**, and Stephen Bliss Utibe-Abasi. (2020). "Analysis Of Obstruction Shadowing In Bullington Double Knife Edge Diffraction Loss Computation." *Journal of Multidisciplinary Engineering Science Studies (JMEST) Vol. 6 Issue 1, January – 2020*
16. Maxama, X. B., & Markus, E. D. (2018, October). A survey on propagation challenges in wireless communication networks over irregular terrains. In *2018 Open Innovations Conference (OI)* (pp. 79-86). IEEE.
17. **Simeon, Ozuomba**, Ezuruike Okafor SF, and Bankole Morakinyo Olumide (2018). Development of Mathematical Models and Algorithms for Exact Radius of Curvature Used in Rounded Edge Diffraction Loss Computation. Development, 5(12). *Journal of Multidisciplinary Engineering Science and Technology (JMEST) Vol. 5 Issue 12, December – 2018*
18. Enoch, S., & Otung, I. (2008, September). Propagation effects in WiMAX systems. In *2008 The Second International Conference on Next Generation Mobile Applications, Services, and Technologies* (pp. 425-430). IEEE.
19. Dialoke, Ikenna Calistus, **Ozuomba Simeon**, and Henry Akpan Jacob. (2020) "ANALYSIS OF SINGLE KNIFE EDGE DIFFRACTION LOSS FOR A FIXED TERRESTRIAL LINE-OF-SIGHT MICROWAVE COMMUNICATION LINK." *Journal of Multidisciplinary Engineering Science and Technology (JMEST) Vol. 7 Issue 2, February - 2020*
20. Coldrey, M., Berg, J. E., Manholm, L., Larsson, C., & Hansryd, J. (2013). Non-line-of-sight small cell backhauling using microwave technology. *IEEE Communications Magazine*, 51(9), 78-84.
21. Samuel, Wali, **Simeon Ozuomba**, and Philip M. Asuquo (2019). EVALUATION OF WIRELESS SENSOR NETWORK CLUSTER HEAD SELECTION FOR DIFFERENT PROPAGATION ENVIRONMENTS BASED ON LEE PATH LOSS MODEL AND K-MEANS ALGORITHM. EVALUATION, 3(11). *Science and Technology Publishing (SCI & TECH) Vol. 3 Issue 11, November - 2019*
22. Sarkar, T. K., Ji, Z., Kim, K., Medouri, A., & Salazar-Palma, M. (2003). A survey of various propagation models for mobile communication. *IEEE Antennas and propagation Magazine*, 45(3), 51-82.
23. Anusha, V. S., Nithya, G. K., & Rao, S. N. (2017, April). A comprehensive survey of electromagnetic propagation models. In *2017 International Conference on Communication and Signal Processing (ICCSP)* (pp. 1457-1462). IEEE.
24. Samuel, W., **Ozuomba, Simeon**, & Constance, K. (2019). SELF-ORGANIZING MAP (SOM)

- CLUSTERING OF 868 MHZ WIRELESS SENSOR NETWORK NODES BASED ON EGI PATHLOSS MODEL COMPUTED RECEIVED SIGNAL STRENGTH. *Journal of Multidisciplinary Engineering Science and Technology (JMEST) Vol. 6 Issue 12, December – 2019*
25. Underhill, M. J. (2003). The estimation and measurement of the efficiency and effectiveness of small antennas in an environment.
 26. Njoku, Felix A., **Ozuomba Simeon**, and Fina Otsi Faithpraise (2019). Development Of Fuzzy Inference System (FIS) For Detection Of Outliers In Data Streams Of Wireless Sensor Networks. *International Multilingual Journal of Science and Technology (IMJST) Vol. 4 Issue 10, October - 2019*
 27. Giggenbach, D., & Henniger, H. (2008). Fading-loss assessment in atmospheric free-space optical communication links with on-off keying. *Optical Engineering*, 47(4), 046001.
 28. Simeon, **Ozuomba**. (2020). "APPLICATION OF KMEANS CLUSTERING ALGORITHM FOR SELECTION OF RELAY NODES IN WIRELESS SENSOR NETWORK." *International Multilingual Journal of Science and Technology (IMJST) Vol. 5 Issue 6, June – 2020*
 29. Speth, M., Fechtel, S. A., Fock, G., & Meyr, H. (1999). Optimum receiver design for wireless broad-band systems using OFDM. I. *IEEE Transactions on communications*, 47(11), 1668-1677.
 30. Simeon, **Ozuomba**. (2020). "Analysis Of Effective Transmission Range Based On Hata Model For Wireless Sensor Networks In The C-Band And Ku-Band." *Journal of Multidisciplinary Engineering Science and Technology (JMEST) Vol. 7 Issue 12, December - 2020*
 31. Alsamhi, S. H., Almalki, F., Ma, O., Ansari, M. S., & Lee, B. (2021). Predictive estimation of optimal signal strength from drones over IoT frameworks in smart cities. *IEEE Transactions on Mobile Computing*.
 32. Allsebrook, K. E. I. T. H., & Parsons, J. D. (1977). Mobile radio propagation in British cities at frequencies in the VHF and UHF bands. *IEEE Transactions on Vehicular Technology*, 26(4), 313-323.
 33. Ozuomba Simeon (2019) Evaluation Of Optimal Transmission Range Of Wireless Signal On Different Terrains Based On Ericsson Path Loss Model Vol. 3 Issue 12, December – 2019 Available at : <http://www.scitechpub.org/wp-content/uploads/2021/03/SCITECHP420157.pdf>
 34. Cardwell, N., Cheng, Y., Gunn, C. S., Yeganeh, S. H., & Jacobson, V. (2016). Bbr: Congestion-based congestion control: Measuring bottleneck bandwidth and round-trip propagation time. *Queue*, 14(5), 20-53.
 35. Johnson, Enyenihi Henry, **Simeon Ozuomba**, and Ifiok Okon Asuquo. (2019). Determination of Wireless Communication Links Optimal Transmission Range Using Improved Bisection Algorithm. *Universal Journal of Communications and Network*, 7(1), 9-20.
 36. Zhang, R., Regunathan, S. L., & Rose, K. (2000). Video coding with optimal inter/intra-mode switching for packet loss resilience. *IEEE Journal on selected areas in communications*, 18(6), 966-976.
 37. Medina, C., Segura, J. C., & Holm, S. (2012, November). Feasibility of ultrasound positioning based on signal strength. In *2012 International Conference on Indoor Positioning and Indoor Navigation (IPIN)* (pp. 1-9). IEEE.
 38. **Simeon, Ozuomba** (2014) "Fixed Point Iteration Computation Of Nominal Mean Motion And Semi Major Axis Of Artificial Satellite Orbiting An Oblate Earth." *Journal of Multidisciplinary Engineering Science and Technology (JMEST) Vol. 1 Issue 4, November – 2014*
 39. Surajudeen-Bakinde, N. T., Faruk, N., Popoola, S. I., Salman, M. A., Oloyede, A. A., Olawoyin, L. A., & Calafate, C. T. (2018). Path loss predictions for multi-transmitter radio propagation in VHF bands using Adaptive Neuro-Fuzzy Inference System. *Engineering Science and Technology, an International Journal*, 21(4), 679-691.
 40. Anower, M. (2012). *Estimation using cross-correlation in a communications network* (Doctoral dissertation, UNSW Sydney).
 41. **Simeon, Ozuomba**. (2016) "Comparative Analysis Of Rain Attenuation In Satellite Communication Link For Different Polarization Options." *Journal of Multidisciplinary Engineering Science and Technology (JMEST) Vol. 3 Issue 6, June – 2016*
 42. Schenato, L., Sinopoli, B., Franceschetti, M., Poolla, K., & Sastry, S. S. (2007). Foundations of control and estimation over lossy networks. *Proceedings of the IEEE*, 95(1), 163-187.
 43. Alves, T., Poussot, B., & Laheurte, J. M. (2010). Analytical propagation modeling of BAN channels based on the creeping-wave theory. *IEEE Transactions on Antennas and Propagation*, 59(4), 1269-1274.
 44. **Simeon, Ozuomba**. (2017). "Determination Of The Clear Sky Composite Carrier To Noise Ratio For Ku-Band Digital Video Satellite Link" *Science and Technology Publishing (SCI & TECH) Vol. 1 Issue 7, July – 2017*

45. Alexiou, A., & Haardt, M. (2004). Smart antenna technologies for future wireless systems: trends and challenges. *IEEE communications Magazine*, 42(9), 90-97.
46. Xia, H. H. (1997). A simplified analytical model for predicting path loss in urban and suburban environments. *IEEE Transactions on Vehicular Technology*, 46(4), 1040-1046.
47. Sharma, P. K., & Singh, R. K. (2010). Comparative analysis of propagation path loss models with field measured data. *International Journal of Engineering Science and Technology*, 2(6), 2008-2013.
48. Popoola, S. I., & Oseni, O. F. (2014). Empirical path loss models for GSM network deployment in Makurdi, Nigeria. *International Refereed Journal of Engineering and Science*, 3(6), 85-94.
49. Seidel, S. Y., & Rappaport, T. S. (1992). 914 MHz path loss prediction models for indoor wireless communications in multifloored buildings. *IEEE transactions on Antennas and Propagation*, 40(2), 207-217.
50. Xia, H. H. (1996, October). An analytical model for predicting path loss in urban and suburban environments. In *Proceedings of PIMRC'96-7th International Symposium on Personal, Indoor, and Mobile Communications* (Vol. 1, pp. 19-23). IEEE.
51. Durgin, G., Rappaport, T. S., & Xu, H. (1998). Measurements and models for radio path loss and penetration loss in and around homes and trees at 5.85 GHz. *IEEE Transactions on communications*, 46(11), 1484-1496.
52. MacCartney, G. R., Zhang, J., Nie, S., & Rappaport, T. S. (2013, December). Path loss models for 5G millimeter wave propagation channels in urban microcells. In *2013 IEEE global communications conference (GLOBECOM)* (pp. 3948-3953). IEEE.
53. Abhayawardhana, V. S., Wassell, I. J., Crosby, D., Sellars, M. P., & Brown, M. G. (2005, May). Comparison of empirical propagation path loss models for fixed wireless access systems. In *2005 IEEE 61st Vehicular Technology Conference* (Vol. 1, pp. 73-77). IEEE.
54. Sevgi, L. (2007). Groundwave modeling and simulation strategies and path loss prediction virtual tools. *IEEE Transactions on Antennas and Propagation*, 55(6), 1591-1598.
55. Ghassemzadeh, S. S., Jana, R., Rice, C. W., Turin, W., & Tarokh, V. (2002, May). A statistical path loss model for in-home UWB channels. In *2002 IEEE Conference on Ultra Wideband Systems and Technologies (IEEE Cat. No. 02EX580)* (pp. 59-64). IEEE.
56. Linka, H., Rademacher, M., Aliu, O. G., & Jonas, K. (2018). Path loss models for low-power wide-area networks: Experimental results using LoRa.
57. Eichie, J. O., Oyedum, O. D., Ajewole, M., & Aibinu, A. M. (2017). Comparative analysis of basic models and artificial neural network based model for path loss prediction. *Progress In Electromagnetics Research M*, 61, 133-146.
58. Phillips, C., Sicker, D., & Grunwald, D. (2011, May). Bounding the error of path loss models. In *2011 IEEE International Symposium on Dynamic Spectrum Access Networks (DySPAN)* (pp. 71-82). IEEE.
59. Imperatore, P., Salvadori, E., & Chlamtac, I. (2007, May). Path loss measurements at 3.5 GHz: a trial test WiMAX based in rural environment. In *2007 3rd International Conference on Testbeds and Research Infrastructure for the Development of Networks and Communities* (pp. 1-8). IEEE.
60. Jo, H. S., Park, C., Lee, E., Choi, H. K., & Park, J. (2020). Path loss prediction based on machine learning techniques: Principal component analysis, artificial neural network, and Gaussian process. *Sensors*, 20(7), 1927.
61. Joseph, I., & Konyeha, C. C. (2013). Urban area path loss propagation prediction and optimisation using hata model at 800mhz. *IOSR Journal of Applied Physics (IOSR-JAP)*, 3(4), 8-18.
62. Nisirat, M. A., Ismail, M., Nissirat, L. A., & Alkhalwaldeh, S. (2011). A terrain roughness correction factor for hata path loss model at 900 MHz. *Progress In Electromagnetics Research C*, 22, 11-22.
63. Roslee, M. B., & Kwan, K. F. (2010). Optimization of Hata propagation prediction model in suburban area in Malaysia. *Progress In Electromagnetics Research C*, 13, 91-106.
64. Nadir, Z., Elfadhil, N., & Touati, F. (2008, July). Pathloss determination using Okumura-Hata model and spline interpolation for missing data for Oman. In *Proceedings of the world congress on Engineering* (Vol. 1, pp. 2-4). London London, UK.
65. Singh, Y. (2012). Comparison of okumura, hata and cost-231 models on the basis of path loss and signal strength. *International journal of computer applications*, 59(11).
66. Banimehem, O., Al-Zu'bi, M. M., & Al Salameh, M. S. (2015, October). Hata path loss model tuning for cellular networks in Irbid City. In *2015 IEEE International Conference on Computer and Information Technology; Ubiquitous Computing and Communications; Dependable, Autonomic and Secure Computing; Pervasive Intelligence and Computing* (pp. 1646-1650). IEEE.
67. Mardeni, R., & Priya, T. S. (2010). Optimised COST-231 Hata models for WiMAX path loss prediction in suburban and open urban environments. *Modern Applied Science*, 4(9), 75.

68. Singh, Y. (2012). Comparison of okumura, hata and cost-231 models on the basis of path loss and signal strength. *International journal of computer applications*, 59(11).
69. Joseph, I., & Konyeha, C. C. (2013). Urban area path loss propagation prediction and optimisation using hata model at 800mhz. *IOSR Journal of Applied Physics (IOSR-JAP)*, 3(4), 8-18.
70. Milanovic, J., Rimac-Drlje, S., & Bejuk, K. (2007, December). Comparison of propagation models accuracy for WiMAX on 3.5 GHz. In *2007 14th IEEE international conference on electronics, circuits and systems* (pp. 111-114). IEEE.
71. Alim, M. A., Rahman, M. M., Hossain, M. M., & Nahid, A. A. (2010). Analysis of large scale propagation models for mobile communications in urban area. *arXiv preprint arXiv:1002.2187*.
72. Dalela, C., Prasad, M. V. S. N., & Dalela, P. K. (2012). Tuning of COST-231 Hata model for radio wave propagation predictions. *Academy & Industry Research Collaboration Center*.
73. Singh, Y. (2012). Comparison of okumura, hata and cost-231 models on the basis of path loss and signal strength. *International journal of computer applications*, 59(11).
74. Nkordeh, N., Atayero, A. A., Idachaba, F. E., & Oni, O. O. (2014). Lte network planning using the hata-okumura and the cost-231 hata pathloss models.
75. Akhpashev, R. V., & Andreev, A. V. (2016, June). COST 231 Hata adaptation model for urban conditions in LTE networks. In *2016 17th International Conference of Young Specialists on Micro/Nanotechnologies and Electron Devices (EDM)* (pp. 64-66). IEEE.
76. Verma, R., & Saini, G. (2016, March). Statistical tuning of Cost-231 Hata model at 1.8 GHz over dense urban areas of Ghaziabad. In *2016 3rd International Conference on Computing for Sustainable Global Development (INDIACom)* (pp. 1220-1225). IEEE.
77. Adekunle, A., Abimiku, Y. K., Umeobika, N. M., & Ameh, E. E. (2018). Radio wave detection using cost 231-Hata model for wireless network planning; a case study of senate building environs of Unilag, Nigeria. *Nigeria IJASRE*, 4.
78. Akinwale, B. O. H., & Esobinwu, C. S. (2013). Adjustment of Cost 231 Hata Path Model For Cellular Transmission in Rivers State. *IOSR J. Electr. Electron. Eng*, 6(5), 16-23.
79. Gulyaeva, T. L., & Rawer, K. (2003). North-south asymmetry of the equatorial anomaly: A model study. *Advances in Space Research*, 31(3), 549-554.
80. Hoque, M. M., & Jakowski, N. (2012, May). A new global model for the ionospheric F2 peak height for radio wave propagation. In *Annales Geophysicae* (Vol. 30, No. 5, pp. 797-809). Copernicus GmbH.
81. Chimaobi, N. N., & Ifeanyi ChimaNnadi, C. P. N. (2017). Comparative Study of Least Square Methods for Tuning CCIR Path Loss Model. *Communications*, 5(3), 19-23.
82. Stephen, M. A., David, O. O., & Oludare, A. M. (2018). Adaptation of Path Loss Models for Terrestrial Broadcast in VHF Band in Minna City, Niger State, Nigeria. *IUP Journal of Telecommunications*, 10(3), 7-24.
83. Afrić, W., & Pilinsky, S. Z. (2012, September). UMTS LTE downlink cell size calculation. In *Proceedings ELMAR-2012* (pp. 105-108). IEEE.
84. Nnadi, N. C., Nnadi, I. C., & Nnadi, C. C. (2017). Optimization of CCIR pathloss model using terrain roughness parameter. *Mathematical and Software Engineering*, 3(1), 156-163.
85. Udofia, K. M. COMPARATIVE ANALYSIS OF OPTIMAL TRANSMISSION RANGE OF Ka-BAND COMMUNICATION LINK BASED ON DIFFERENT DEGREES OF URBANIZATION IN CCIR PATH LOSS MODEL.
86. Prasad, M. V. S. N., Sain, M., & Reddy, B. M. (1990). Effect of obstacles on VHF TV signal propagation. *IEEE transactions on broadcasting*, 36(3), 234-241.
87. Haralambous, H., Leontiou, T., Petrou, V., Kumar Singh, A., Charalambides, M., Lithoxopoulos, N., & Agisilaou, A. (2021). Adjusting CCIR Maps to Improve Local Behaviour of Ionospheric Models. *Atmosphere*, 12(6), 691.
88. Haralambous, H., Leontiou, T., Petrou, V., Kumar Singh, A., Charalambides, M., Lithoxopoulos, N., & Agisilaou, A. (2021). Adjusting CCIR Maps to Improve Local Behaviour of Ionospheric Models. *Atmosphere*, 12(6), 691.
89. Neskovic, A., Neskovic, N., & Paunovic, D. (2002). Macrocell electric field strength prediction model based upon artificial neural networks. *IEEE Journal on selected areas in Communications*, 20(6), 1170-1177.